

# UC Davis

## UC Davis Previously Published Works

### Title

Optical observation of lipid- and polymer-shelled ultrasound microbubble contrast agents

### Permalink

<https://escholarship.org/uc/item/1bd0x386>

### Journal

Applied Physics Letters, 84(4)

### ISSN

0003-6951

### Authors

Bloch, Susannah H

Wan, M

Dayton, P A

et al.

### Publication Date

2004

Peer reviewed

## Optical observation of lipid- and polymer-shelled ultrasound microbubble contrast agents

Susannah H. Bloch,<sup>a)</sup> Mingxi Wan, Paul A. Dayton, and Katherine W. Ferrara  
*Department of Biomedical Engineering, University of California at Davis, Davis, California 95616*

(Received 14 May 2003; accepted 25 November 2003)

High-speed optical experiments demonstrate that the behavior of a polymer-shelled microbubble contrast agent in response to an acoustic pulse is qualitatively and quantitatively different from that of a lipid-shelled agent. The lipid-shelled agent expands in response to a two-cycle pulse, and at pressures approaching 1 MPa, both the shell and its contents fragment. The polymer-shelled agent remains largely intact at pressures up to 1.5 MPa and exhibits a different destruction mechanism: the polymer shell does not oscillate significantly in response to ultrasound; instead, a gas bubble is extruded and ejected through a shell defect while the shell appears to remain largely intact. © 2004 American Institute of Physics. [DOI: 10.1063/1.1643544]

Ultrasound microbubble contrast agents are used to increase ultrasound backscatter from blood, enabling imaging of capillary networks,<sup>1,2</sup> as well as new techniques for drug delivery<sup>3</sup> and targeted imaging.<sup>4</sup> Currently there are at least 20 such agents under development.<sup>5</sup> The agents can be filled with air or with low-solubility gases such as sulfur hexafluoride or perfluorocarbons, or can be liquid droplets that change phase at body temperature; their shells can be composed of lipids, albumin, or polymer. Experiments to characterize different agents' behavior in response to ultrasound are an important part of designing agent-specific detection methods and determining the best clinical application for a specific agent. The behavior of lipid- and albumin-shelled agents has been characterized by several researchers;<sup>6,7</sup> polymer-shelled agents are a relatively new development and the research on how their behavior differs from that of other agents is limited.<sup>8-11</sup> Here we compare the behavior of a lipid-shelled ultrasound contrast agent, BR14, and a polymer-shelled ultrasound contrast agent, BG1135, using a high-speed camera capable of visualizing individual contrast microbubble responses to acoustic interrogation in real time.<sup>12</sup>

Vials of agents BR14 and BG1135 were provided by Bracco Research S. A. (Geneva, Switzerland). BR14 is a perfluorobutane-filled microbubble, stabilized by a phospholipid monolayer shell a few nanometers thick. It has a mean diameter of 2.6  $\mu\text{m}$  and 99% of BR14 agents have diameters less than 12  $\mu\text{m}$ . BG1135 is an air-filled microsphere with a rigid, 100 nm thick polymeric shell and a mean diameter of 2.9  $\mu\text{m}$  (99% less than 8  $\mu\text{m}$ ).

The procedure for high-speed photography of microbubbles employed by our group has been described extensively in previous publications.<sup>11-15</sup> Briefly, a high-speed camera (Imacon 468, DRS Hadland Inc.) interfaced to a custom microscope (Mikron Instruments IV500L) was used to capture still and streak images of individual microbubbles. The microscope was fitted with a 100 $\times$  water-submersible objective (Zeiss Achroplan 100 $\times$ , Carl Zeiss Microimaging

Inc.) and 1.6 $\times$  zoom. A water tank with a spherically focused 2.25 MHz transducer (V305, Panametrics Inc., focal length 5.94 cm, 3 dB beam width 1.2 mm) mounted in one wall was located below the objective such that the optical and acoustical focal volumes overlapped. A 200  $\mu\text{m}$  i.d. cellulose tube (Spectrum Labs Inc.), which is nearly optically and acoustically transparent, was placed into this mutual focus. The tube was placed parallel to the bottom of the water bath and perpendicular to the beam axis of the transducer. Contrast agent solution was pumped through the tube with a manual microinjector (IM-5B, Narishige International USA Inc.). The microbubbles in the tube could thus be observed optically during exposure to acoustic pulses generated by the transducer, which was driven by a signal from an arbitrary wave form generator (AWG 2021, Tektronix Inc.) amplified approximately 55 dB with a rf amplifier (3100LA, MKS ENI Products).

The transducer was calibrated with a needle hydrophone (PZT-Z44-0200, Specialty Engineering Associates) and a preamplifier (A17DB Specialty Engineering Associates) connected to an oscilloscope. The tip of the needle hydrophone was positioned in the optical field of view so that the pressure measured was the same as that experienced by agents in the optical field of view. The optical system was calibrated using a calibration reticle, yielding a resolution of 7.5 pixels/ $\mu\text{m}$ .

Both types of agents were diluted until optical observation confirmed approximately one bubble per optical field of view (a maximum concentration of 2500 bubbles/ $\mu\text{l}$ ). The agents were exposed to 2.25 MHz, two-cycle pulses at peak negative pressures ranging from 180 kPa to 1.42 MPa. The streak images were collected with a streak slit 50  $\mu\text{m}$  wide and a streak speed (duration of streak) of 5  $\mu\text{s}$  (a line sampling frequency of 100 MHz). The frame and streak timing were set such that the agent was observed before, during, and after exposure to the ultrasound pulse; the exposure times were set to 50 ns for frames taken during agent motion and 500 ns otherwise.

Approximately 40 image sets (seven still images and a streak image) were obtained for each of the two contrast agent types at each of three pressures. For each set, measure-

<sup>a)</sup>Electronic mail: shbloch@ucdavis.edu

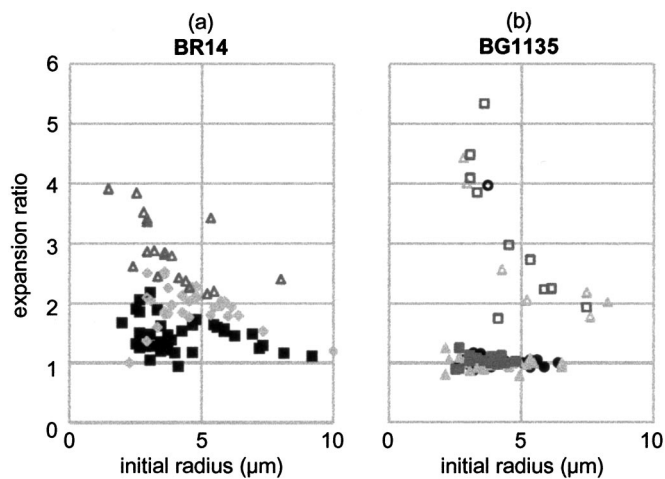


FIG. 1. Expansion ratio ( $r_{\max}/r_0$ ) vs initial radius ( $r_0$ ) in response to a two-cycle, 2.25 MHz pulse for (a) BR14 (squares, 180 kPa; diamonds, 360 kPa; triangles, 920 kPa) and (b) BG1135 (circles, 660 kPa; triangles, 1.2 MPa; squares, 1.4 MPa). Closed symbols indicate agents that remained intact after insonation; open symbols indicate those agents that fragmented in response to the ultrasound pulse.

ments were made on the streak image of initial, maximum, and final agent diameter, and a subjective decision was made about whether or not the agent had “fragmented,” or split into two or more entities,<sup>12,15</sup> during the acoustic pulse by inspecting the still and streak images. Contrast agent fragmentation depended on agent type, initial radius, and applied pressure (Fig. 1).

We observed four differences between the lipid-shelled agent, BR14, and the polymer-shelled agent, BG1135. BR14 was similar to other lipid-shelled agents:<sup>12</sup> the agent appeared to have a spherical shape and uniform shell; it was destroyed consistently by pulses of 920 kPa at 2.25 MHz (19 of 19 BR14 agents fragmented); its shell oscillated in response to ultrasound and fragmented along with its gas contents when the agent was destroyed; and it also exhibited a reduction in diameter due to acoustically-driven diffusion<sup>15</sup> in response to nondestructive ultrasound pulses. BG1135 often appeared under magnification to have a nonspherical shape or nonuniform shell [as in Fig. 3(e)]. Under 2.25 MHz insonation, it remained largely intact at pressures up to 500 kPa above those at which BR14 was consistently fragmented (only 5 of 14 BG1135 agents were fragmented by 1.54 MPa, 2.25 MHz pulses). There was no evidence of significant oscillation of the agent shell either before or after fragmentation [on average no more than 5%, Fig. 3(h)], and we observed no evidence of a change in diameter in cases where the BG1135 agent did not fragment.

In a typical case of BR14 destruction (Fig. 2), the agent shell collapses during the compressional phase of the ultrasound pulse, and upon re-expansion the agent and its contents are fragmented into several pieces that are centered around the starting position of the agent. BG1135, on the other hand, often appeared to acquire a small shell defect, allowing gas to stream out and creating a new gas bubble, but leaving the old shell intact (Fig. 3)—there was no significant difference between the diameter of the shell measured before and after insonation ( $P=0.55$ ,  $n=17$ ), even though the agent had fragmented. The wall velocity of the

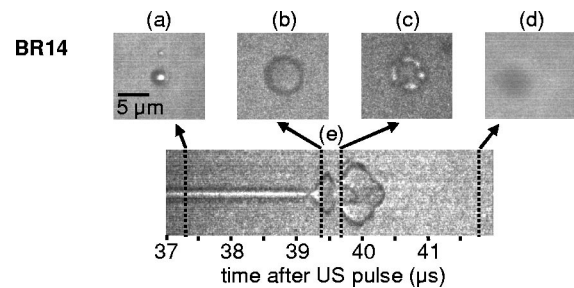


FIG. 2. Destruction of BR14. Still images (a)–(d) depict the agent before, during, and after exposure to a two-cycle, 2.25 MHz, 920 kPa ultrasound pulse. Streak image (e) shows one line of sight through the agent vs time, with the acquisition times of the still images indicated by dotted lines. The agent is observed to expand and collapse in response to the ultrasound pulse. During the second cycle, fragments of the agent expand again around the position of the original agent.

expanding gas bubble edge, measured from the streak image, was  $28 \pm 6 \mu\text{m}/\mu\text{s}$  ( $n=17$ ). The new gas bubble was often ejected some distance from the agent shell (Fig. 3). The gas bubble ejection did not occur preferentially in the image plane and so was not observed in all cases. In the six cases where a new gas bubble was visible in the final image and its trajectory could be traced along the streak image, the gas bubble appeared to expand through a defect or crack in the agent shell in response to the rarefaction cycle of the ultrasound pulse, then move away from the shell at a velocity of up to  $10 \mu\text{m}/\mu\text{s}$  for 1–2  $\mu\text{s}$ . The mean radius of the gas bubble after insonation was  $3.4 \pm 1.3 \mu\text{m}$  (compared with a shell radius of  $5.7 \pm 1.6 \mu\text{m}$ ), and the bubbles were located as far as  $10 \mu\text{m}$  away from the original shell. In seven cases, the

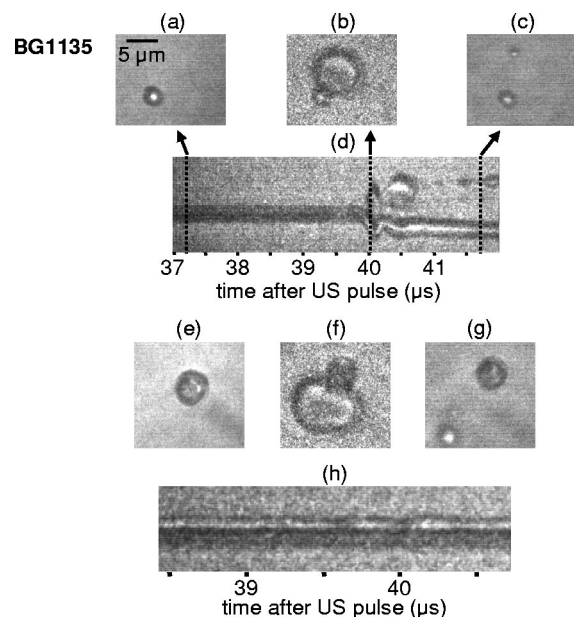


FIG. 3. Destruction of BG1135. Still images (a)–(c) depict the agent before, during, and after exposure to a two-cycle, 2.25 MHz, 1.4 MPa ultrasound pulse. Streak image (d) shows one line of sight through the agent vs time, with the acquisition times of the still images indicated. The agent is observed to acquire a shell defect and subsequently to eject a gas bubble some distance from the original shell. Images (e)–(g) show destruction of another BG1135 agent in response to a two-cycle, 2.25 MHz, 1.2 MPa pulse. Image (h) shows very slight oscillation of a BG1135 agent in response to a two-cycle, 2.25 MHz, 1.4 MPa pulse. This is the largest oscillation we observed in an unfragmented agent under these conditions.

shell appeared to be displaced slightly (2–4  $\mu\text{m}$ ) by the expanding bubble.

The destruction mechanism of BG1135 is unique among the agents we have studied. We have previously reported ejection of a gas bubble through a shell defect in Optison agents, which have a semirigid albumin shell,<sup>14</sup> but in that experiment we observed that the resulting gas bubble moved away from the shell much more slowly (traveling several microns in milliseconds instead of microseconds), and that the shell collapsed after the gas bubble was ejected. The mechanism of gas bubble extrusion, ejection, and displacement several bubble diameters away from the BG1135 agent shell is not known and not accounted for by current bubble models.<sup>15</sup> The velocities involved, on the order of meters per second, are slow compared to studies of bubble jets injected into a liquid.<sup>16</sup> We also do not believe the gas bubbles were driven away from the shell by radiation force because they did not move preferentially along the acoustic axis.

It is possible to speculate on the practical consequences of these optically observed behavior differences. The inflexibility of the BG1135 shell may make it more difficult to detect acoustically under nondestructive conditions and not appropriate for low-pressure harmonic or subharmonic imaging. Conversely, it might be ideal for an application where low-amplitude tissue-imaging pulses were used before a release “burst” to determine the location of the contrast agent,<sup>17</sup> as in stimulated acoustic emission imaging of the liver.<sup>18</sup> The imaging-release-imaging sequence frames could be closely spaced, since the gas bubble is formed and escapes the shell on a time scale of microseconds. More acoustical experiments, both in the laboratory and *in vivo*, will be required to confirm these hypotheses, but the optical experiments reported here have given us insight into the difference in behavior between the two agents. Further research would be necessary to develop a model that will correctly predict the acoustic response and destruction threshold of this polymer-shelled agent.

This work was made possible by funding from Bracco Research SA and NIH Grant No. CA76062, and by the assistance of Peter Frinking of Bracco Research.

- <sup>1</sup>B. B. Goldberg, J. B. Liu, and F. Forsberg, *Ultrasound Med. Biol.* **20**, 319 (1994).
- <sup>2</sup>K. W. Ferrara, C. R. Merritt, P. N. Burns, F. S. Foster, R. F. Mattrey, and S. A. Wickline, *Acad. Radiol.* **7**, 824 (2000).
- <sup>3</sup>R. J. Price and S. Kaul, *J. Cardiovasc. Pharmacol. Ther.* **7**, 171 (2002).
- <sup>4</sup>P. A. Dayton and K. W. Ferrara, *J. Magn. Reson Imaging* **16**, 362 (2002).
- <sup>5</sup>*Ultrasound Contrast Agents, Basic Principles and Clinical Applications*, edited by B. B. Goldberg, J. S. Raichlen, and F. Forsberg (Dunitz, London, 2001).
- <sup>6</sup>N. de Jong, A. Bouakaz, and P. Frinking, *Echocardiography* **19**, 229 (2002).
- <sup>7</sup>K. E. Morgan, Ph.D. thesis, University of Virginia, Charlottesville, VA, 2001.
- <sup>8</sup>W. S. Chen, T. J. Matula, A. A. Brayman, and L. A. Crum, *J. Acoust. Soc. Am.* **113**, 643 (2003).
- <sup>9</sup>W. S. Chen, T. J. Matula, and L. A. Crum, *Ultrasound Med. Biol.* **28**, 793 (2002).
- <sup>10</sup>K. Ohmori, A. N. DeMaria, B. Cotter, O. L. Kwan, A. Oshita, I. Kondo, K. Mizushige, and M. Kohno, *Ultrasound Med. Biol.* **29**, 279 (2003).
- <sup>11</sup>D. Patel, P. Dayton, J. Gut, E. Wisner, and K. W. Ferrara, *IEEE Trans. Ultrason. Ferroelectr. Freq. Control* **49**, 1641 (2002).
- <sup>12</sup>J. E. Chomas, P. Dayton, D. May, and K. Ferrara, *J. Biomed. Opt.* **6**, 141 (2001).
- <sup>13</sup>P. A. Dayton, J. E. Chomas, A. F. Lum, J. S. Allen, J. R. Lindner, S. I. Simon, and K. W. Ferrara, *Biophys. J.* **80**, 1547 (2001).
- <sup>14</sup>P. A. Dayton, K. E. Morgan, A. L. Kilbanov, G. H. Brandenburger, and K. W. Ferrara, *IEEE Trans. Ultrason. Ferroelectr. Freq. Control* **46**, 220 (1999).
- <sup>15</sup>J. E. Chomas, P. Dayton, J. Allen, K. Morgan, and K. W. Ferrara, *IEEE Trans. Ultrason. Ferroelectr. Freq. Control* **48**, 232 (2001).
- <sup>16</sup>K. Chen and H. J. Richter, *Int. J. Multiphase Flow* **23**, 699 (1997).
- <sup>17</sup>P. J. Frinking, E. I. Cespedes, J. Kirkhorn, H. G. Torp, and N. de Jong, *IEEE Trans. Ultrason. Ferroelectr. Freq. Control* **48**, 643 (2001).
- <sup>18</sup>M. J. Blomley, T. Albrecht, D. O. Cosgrove, R. J. Eckersley, J. Butler-Barnes, V. Jayaram, N. Patel, R. A. Heckemann, A. Bauer, and R. Schlieff, *Ultrasound Med. Biol.* **25**, 1341 (1999).